Doctoral thesis

Effects of chitin nanofibrils on skin

キチンナノファイバーの皮膚への効果

The United Graduate School of Veterinary Science

Yamaguchi University

Ikuko Ito

September 2017

Contents

Page No.

Chapter Ⅱ.

Protective Effect of Chitin Urocanate Nanofibers against Ultraviolet Radiation

Publications

Evaluation of the effects of chitin nanofibrils on skin function using skin models

Ito I, Osaki T, Ifuku S, Saimoto H, Takamori Y, Kurozumi S, Imagawa T, Azuma K, Tsuka T, Okamoto Y, Minami S.

Carbohydrate Polymers, 30 (101), 464~470, 2014

Protective effect of chitin urocanate nanofibers against ultraviolet radiation

Ito I, Yoneda T, Omura Y, Osaki T, Ifuku S, Saimoto H, Azuma K, Imagawa T, Tsuka T, Murahata Y, Ito N, Okamoto Y, Minami S.

Marine Drugs, 13 (12), 7463~7475, 2015

Abstract

Chapter Ⅰ.

Evaluation of the effects of chitin nanofibrils on skin function using skin models

Chitins are highly crystalline structures that are predominantly found in crustacean shells. Alpha-chitin is composed of microfibers, which are made up of nanofibrils (NFs) that are 2–5 nm in diameter and 30 nm in length and embedded in a protein matrix. Crystalline NFs can also be prepared by acid treatment. We verified the effect of chitin NFs and nanocrystals (NCs) on skin using a three-dimensional skin culture model and Franz cells. The application of NFs and NCs to skin improved the epithelial granular layer and increased granular density. Furthermore, NFs and NCs application to the skin resulted in a lower production of TGF-β compared to that of the control group. NFs and NCs might have protective effects to skin. Therefore, their potential use as components of skin-protective formulations merits consideration.

Chapter Ⅱ.

Protective effect of chitin urocanate nanofibers against ultraviolet radiation

Urocanic acid is a major ultraviolet (UV)-absorbing chromophore. Chitins are highly crystalline structures that are found predominantly in crustacean shells. Alpha-chitin consists of microfibers that contain nanofibrils (NFs) embedded in a protein matrix. Acid hydrolysis is a common method used to prepare chitin NFs. We typically obtain NFs by hydrolyzing chitin with acetic acid. However, in the present study, we used urocanic acid to prepare urocanic acid chitin NFs (UNFs) and examined its protective effect against UVB radiation. Hos:HR-1 mice coated with UNF were UVB irradiated (302 nm, 150 mJ/cm^2), and these mice showed markedly lower UVB radiation-induced cutaneous erythema than the control. Additionally, sunburn cells were rarely detected in the epidermis of UNFs-coated mice after UVB irradiation. Although the difference was not as significant as UNFs, the number of sunburn cells in mice treated with acetic acid chitin nanofibrils (ANFs) tended to be lower than in control mice. These results demonstrate that ANFs have a protective effect against UVB and suggest that the anti-inflammatory and antioxidant effects of NFs influence the protective effect of ANF against UVB radiation. The combination of NFs with other substances that possess UV-protective effects, such as urocanic acid, may provide an enhanced protective effect against UVB radiation.

General Introduction

1. Introduction

Alpha-chitin is composed of microfibers, which are made up of nanofibrils (NFs) that are approximately 2–5 nm in diameter and 30 nm in length and embedded in a protein matrix [1, 2, 3]. Isolated chitin NFs show a potential for use in drug delivery systems, the tissue engineering of scaffolds, and wound dressing [4]. Acid hydrolysis is one of the main methods used to prepare chitin NFs [5, 6]. Moreover, ultrasonication of squid pen beta-chitin under acidic conditions yields 3–4-nm-wide chitin NFs with relatively low crystallinity [7]. Chitin nanofibers are easily prepared using either fine grinding or wet-type atomization methods [8].

Chitin and chitosan have an accelerating effect on the wound healing process and regulate immune response [9, 10]. Recently, chitin and chitosan could be used as NFs. However, it is unclear whether chitin NFs could maintain original function or not.

We have previously found that chitin NFs improve the clinical symptoms and suppress the onset of ulcerative colitis in an animal model [11]. Furthermore, chitin NFs suppressed myeloperoxidase activation in the colon and decreased serum interleukin (IL)-6 concentrations. In contrast, the application of chitin powder did not produce any anti-inflammatory effect [11].

Because many people exhibit skin hypersensitivity in response to cosmetics and textiles, the development of materials exempt from inflammatory activity is essential. In the chapter Ⅰ, we describe a novel three-dimensional skin model assay and Franz cells to evaluate the skin-protective effects of chitin NFs. Our results suggested that chitin NFs are mildly irritating to the skin and can protect skin cells. In the chapter Ⅱ, we prepared urocanic acid (UCA) chitin NFs (UNFs) by UCA hydrolysis. We hypothesized that we could generate valuable new NFs with UV-blocking function by preparing NFs with UCA, and we examined the protective effect of the UNFs against UV radiation.

References

[1] P. Y. Chen, A. Y. Lin, J. McKittrick, and M. A. Meyers, Structure and mechanical properties of crab exoskeletons. *Acta Biomaterialia, 4*, 587–596. (2008).

[2] D. Raabe, P. Romano, C. Sachs, H. Fabritius, A. A. Sawalmih, S. B. Yi, G. Servos, and H. G. Hartwig, Microstructure and crystallographic texture of the chitin–protein network in the biological composite material of the exoskeleton of the lobster Homarus americanus. *Materials Science and Engineering*, *421*, 143–153. (2006).

[3] S. Nikolov, H. Fabritius, M. Petrov, M. Friak, L. Lymperakis, C. Sachs, D. Raabe, and J. Neugebauer, Robustness and optimal use of design principles of arthropod exoskeletons studied by ab initio based multiscale simulations. *Journal of The Mechanical Behavior of Biomedical Materials*, 4, 129-145. (2011).

[4] R. A. A. Muzzarelli, P. Morganti, G. Morganti, P. Palombo, M. Palombo, G. Biagini, M. M. Belmonte, F. Giantomassi, F. Orlandi, and C. Muzzarelli, Chitin nanofibrils/chitosan glycolate composites as wound medicaments. *Carbohydrate Polymers*, 70, 274–284. (2007).

[5] N. K. Gopalan and A. Dufresne, Crab shell chitin whisker reinforced 318 natural rubber nanocomposites 1. Processing and swelling behavior. *Biomacromolecules,* 4, 657–665. (2003).

[6] J. F. Revol and R. H. Marchessault, In vitro chiral nematic ordering of chitin crystallites. *International Journal of Biological Macromolecules*, 15, 329–335. (1993).

[7] Y. Fan, T. Saito, and A. Isogai, Preparation of chitin nanofibers from squid pen beta-chitin by simple mechanical treatment under acid conditions. *Biomacromolecules*, 9, 1919-1923. (2008).

[8] S. Ifuku and H. Saimoto, Chitin nanofibers: preparations, modifications, and applications. *Nanoscale*, 4, 3308–3318. (2012).

[9] R. A. A. Muzzarelli, Chitins and chitosans for the repair of wounded skin, nerve, cartilage and bone. *Carbohydrate Polymers*, 76 167-182. (2009).

[10] R. A. A. Muzzarelli, Chitins and chitosans as immunoadjuvants and non-allergenic drug carriers. *Marine Drugs*, 8, 292-312. (2010).

[11] K. Azuma, T. Osaki, T. Wakuda, S. Ifuku, H. Saimoto, T. Tsuka, T. Imagawa, Y. Okamoto, and S. Minami, Beneficial and preventive effect of chitin nanofibrils in a dextran sulfate sodium-induced acute ulcerative colitis model. *Carbohydrate Polymers*, 87, 1399–1403. (2012).

Chapter Ⅰ.

Evaluation of the effects of chitin nanofibrils on skin function using skin models

Abstract

Chitins are highly crystalline structures that are predominantly found in crustacean shells. Alpha-chitin is composed of microfibers, which are made up of nanofibrils (NFs) that are 2–5 nm in diameter and 30 nm in length and embedded in a protein matrix. Crystalline NFs can also be prepared by acid treatment. We verified the effect of chitin NFs and nanocrystals (NCs) on skin using a three-dimensional skin culture model and Franz cells. The application of NFs and NCs to skin improved the epithelial granular layer and increased granular density. Furthermore, NFs and NCs application to the skin resulted in a lower production of TGF-β compared to that of the control group. NFs and NCs might have protective effects to skin. Therefore, their potential use as components of skin-protective formulations merits consideration.

1. Introduction

Alpha-chitin is composed of microfibers, which are made up of NFs that are approximately 2–5 nm in diameter and 30 nm in length and embedded in a protein matrix [1, 2, 3, 4] . Isolated chitin NFs show a potential for use in drug delivery systems, the tissue engineering of scaffolds, and wound dressing [5]. Acid hydrolysis is one of the main methods used to prepare chitin NFs [6, 7]. Moreover,

ultrasonication of squid pen beta-chitin under acidic conditions yields 3–4-nm-wide chitin NFs with relatively low crystallinity [8]. Chitin nanofibers are easily prepared using either fine grinding or wet-type atomization methods [9].

Chitin and chitosan have an accelerating effect on the wound healing process and regulate immune response [10, 11]. Recently, chitin and chitosan could be used as nanofibrils. However, it is unclear whether chitin NFs could maintain original function or not.

We have previously found that chitin NFs improve the clinical symptoms and suppress the onset of ulcerative colitis in an animal model [12]. Furthermore, chitin NFs suppressed myeloperoxidase activation in the colon and decreased serum interleukin (IL)-6 concentrations. In contrast, the application of chitin powder did not produce any anti-inflammatory effect [12].

Because many people exhibit skin hypersensitivity in response to cosmetics and textiles, the development of materials exempt from inflammatory activity is essential. In the present study, we describe a novel three-dimensional skin model assay to evaluate the skin-protective effects of chitin NFs.

2. Materials and methods

2.1. Preparation of chitin nanofibers and chitin nanocrystals

Chitin NFs and NCs were prepared as described previously [6, 13]. In brief, dry chitin powder from crab shell was dispersed in water at 1 wt.%, and acetic acid (AC) was added to adjust the pH value to 3 to facilitate fibrillation. The chitin was roughly crushed with a domestic blender. Finally, the slurry was passed through a grinder (MKCA6–3; Masuko Sangyo Co., Ltd.) at 1500 rpm. Chitin

crystals were prepared by hydrolyzing the chitin with 3 N HCl at the boil for 90 min under stirring. After acid hydrolysis, the suspension was washed with distilled water (DW) by centrifugation thoroughly. The precipitate was dispersed in water at 1 wt.%, and AC was added to adjust the pH value to 3. The chitin was passed through a grinder.

2.2. Test materials

Test using 3D human skin culture model**:** We prepared a 1% chitin NFs dispersion and a 1% chitin NCs dispersion at pH 3 and pH 6 by the grinding method described by Ifuku & Saimoto (2012). Control solutions were DW, or AC at pH 3 and pH 6. 1% N-acetyl-D-glucosamine (GlcNAc) was used as a positive control for effect of the keratinocyte growth factor [14].

Test using Franz diffusion cells**:** We prepared samples of 1% chitin NFs and 1% chitin NCs under the following conditions at pH 6, Ac at pH 6, and DW.

2.3. Test procedures using 3D human skin culture model

The three-dimensional epidermal model LabCyte EPI-MODEL 24 (Tissue Engineering Japan Co, Aichi) was used to test the contact effect of each sample. This model, which includes skin layers between the keratin layer and the basal layer, was incubated at 37°C in a 5% CO_2 humidified atmosphere.

The 9 conditions tested in this experiment are as follows: 1) no application (NON) (n = 8); 2) DW (n = 12); 3) 1% AC solution, pH 3 (n = 8); 4) 1% AC solution, pH 6 (n = 8); 5) 1% chitin NFs dispersed at pH 3 (n = 8); 6) 1% chitin NFs dispersed at pH 6 (n = 12); 7) 1% chitin NCs dispersed at pH 3 (n = 8); 8) 1%

chitin NCs dispersed at pH 6 (n =12); and 9) 1% GlcNAc (n = 12).

The assay media (0.5 mL/well) (Tissue Engineering Japan Co, Aichi) was aliquoted into the assay plate (Tissue Engineering Japan Co, Aichi). Next, the three-dimensional skin culture model was placed in each well. The assay plates were then incubated in a CO_2 incubator for 1 h. The test material (50 μL/well) was applied to the keratin layer of the three-dimensional skin culture model after the 1-h incubation.

The three-dimensional human skin culture models were removed from the assay plate at 4, 12, and 24 h post-application, and the cultured skin (from the keratin to basal layers) were harvested.

2.4. Histological observations

The harvested skin culture was immersed and fixed in 10% formalin (Mildform 10N, Wako Pure Chemical Industries Ltd., Osaka, Japan). Cross-sectional slices (4-μm-thick) were soaked in hematoxylin and eosin (H&E) and histological evaluations were conducted. The samples were prepared by Sumika Technoservice Corporation (Osaka, Japan). The H&E stained samples from each experimental group were evaluated using an optical microscope (BX51-FL, Olympus Corporation, Tokyo). The tissue image analysis was done using Lumina Vision (Ver. 2.5.2.1, Mitani Corporation, Tokyo, Japan).

Images for 4 non-continuous fields of view at 400 × magnification were taken for each H&E-stained sample in each experimental group. Sample scores were calculated by averaging the observational scores from one quadrant of the image for the granular layer and stratum spinosum. The below criteria were used to

convert the observations into a score.

2.5. Assessment of the granular layer and the stratum spinosum

The number of granular layers and the granule cell density of the layers were evaluated.

A complete absence of the granular layer was assigned a score of 0; a partial granular layer was assigned a score of 1; if 1, 2, 3, or 4 layers were present, scores of 2, 3, 4, and 5, respectively, were assigned.

The granule cells lacking keratohyalin granules were assigned a score of 0, a weak presence was assigned a score of 1, a moderate abundance with a high dye-affinity was assigned a score of 2, and a granule cell with abundant granules was assigned a score of 3.

The stratum spinosum quality was evaluated by measuring the width of the intercellular gap and the clarity of the nucleus. A score of 0 was assigned if the intercellular contacts in the stratum spinosum had collapsed; 1, if the intercellular gap was greater than 1 mm at 400 × magnification; 2, if the space was less than 1 mm; and 3, if a space could not be confirmed by the naked eye, when I displayed the image which photographed at magnification 400 times with 122 mm in height, size of 163 mm in width In addition, a score of 1 was assigned if the nucleus was clearly visible; otherwise, a score of 2 was assigned.

2.6. Test procedures using Franz diffusion cells

Franz diffusion cells (PermeGear Inc., Keystone Scientific K.K., Japan) were used to evaluate the test model. Skin removed from Hos:HR-1 mice (8–9 wk-old,

25–35-g males, Hoshino Laboratory Animals, Inc., Ibaraki, Japan) was used. The use of the animals and the procedures they underwent were approved by the Animal Research Committee of Tottori University.

The 4 experimental conditions were as follows: 1) DW (n = 4); 2) 1% AC solutions of pH 6 (n = 4); 3) 1% chitin NFs dispersed at pH 6 (n = 4); and 4) 1% chitin NCs dispersed at pH 6 (n = 4).

Skin samples removed from mice sacrificed by cervical dislocation were applied to 1X phosphate buffered saline (PBS 10X, pH 7.4; Life Technologies Corporation, Tokyo, Japan)-soaked Franz cells. The cells were incubated in a thermostat chamber for 1 h (TERMO MINDER EX; Taitec Corporation, Saitama, Japan). Each test material was then applied and the cells were re-incubated. A graphical illustration of the methods is shown in Figure 1.

At 1, 3, and 6 h post-application, PBS was aspirated from the cells. Approximately 1 and 3 h after removal of PBS, fresh PBS was injected into Franz cells using a disposable feeding needle (FG6206; Fuchigami, Kyoto, Japan), and reincubated. The aspirated PBS was concentrated using a centrifuge (SCT 5BA, Hitachi Koki Co. Ltd., Tokyo) at 4,000 *g* for 20 min at room temperature. The concentrated PBS was stored at -80°C until analysis.

2.7. Measurement of cytokine concentrations in PBS

We measured the concentration of IL-1α and TGF-β using a commercially available cytokine measurement kit (Mouse, ELISA Kit, Quantikine M (96 well), R&D Systems, Minneapolis, USA). In addition, we calculated the cumulative cytokine production level through the summation of cytokine concentrations at

each time point.

2.8. Statistical analysis

Analysis was performed using 4step Excel Statistics (OMS Publishing, Saitama, Japan). For each investigation, we performed the Bartlett test for normality; for those where we confirmed normality or equal variance, single factor ANOVA was performed; otherwise, we used the Kruskal-Wallis test. Afterwards, a multiple comparison test (the Tukey-Kramer test or Scheffe's F test) was performed. A risk ratio of less than 5% ($p < 0.05$) was considered significant. A risk ratio less than 1% ($p < 0.01$) was considered highly significant.

3. Results

3.1. Experiment 1: Effect of chitin NFs on epithelial cells using a three-dimensional skin culture model

Histological observations for each group are shown in Table 1. In the NON group, the granular layer score was 2.5 and granule cell concentrations score was maintained at 1.9 points 24 h post-application. However, the intercellular gap and nucleus clarity scores were relatively low (0.2–0.4 points and 0.3–0.4 points, respectively) 12 h post-application.

In the DW-treated group, the granular layer score was over 2.5 until 4 h post-application, after which time, it fell below 2.5 and was very low 24-h post-application, and the granule cell density and intercellular gap scores 24 h post-application were low (1.1 and 0.2 points, respectively).

In the AC (pH 3) group, the granular layer scores 12 h post-application were

2.5, and gradually decreased below 2.5 points by 24 h post-application. The granule cell density score was 1.3 points 12 h post-application and 1.1 points 24 h post-application.

In the Ac (pH 6) group, although the granular layer score was below 2.5 at 24 h post-application, scores for granule cell density (1.5 points), intercellular gap (0.7 point) and nucleus clarity (0.9 points) indicated good results.

In the NFs (pH 3) group, the granular layer scores 4 h post-application were above 2.5; however, they subsequently decreased by 12 h post-application. Similarly, the granule cell density scores were high (1.9 points) 4 h post-application, but subsequently fell to 0.8–1.3 points by 12 h post-application. The intercellular gap and nucleus clarity scores were favorable 12 h post-application (1.3–1.6 and 1.0 points, respectively).

At all measured time points, the granular layer scores for the NFs (pH 6) group were over 2.5, and the scores for granule cell density (1.7–2.5 points), intercellular gap (1.0–1.3 points), and nucleus clarity (0.9–1.0 points) were also maintained at satisfactory values post-application.

Granular layer scores for the NC (pH 3) group fell below 2.5 points beginning 12 h post-application. Granule cell scores were also low (0.5–1.2 points) after this time. Both the intercellular gap and nucleus clarity scores remained constant (1 point) at all the measured time points.

Similar to the NFs (pH 6) group, the granular layer scores for the NCs (pH 6) group were above 2.5 at all measured time points. Additionally, scores for granule cell concentrations (1.7–2.1 points), intercellular gap (1.4–1.9 points), and nucleus clarity (0.9–1.0 points) remained satisfactory post-application.

In the GlcNAc group, all measured values were satisfactory until 12 h post-application; however, 24 h post-application, scores for the granular layer fell below 2.5, while granule cell density and intercellular gap scores were low, at 1.0 and 0.6 points, respectively.

Comparisons for each group are shown in Figure 2. Furthermore, histological images for the NON, DW, NCs (pH 6), and NFs (pH 6) groups 24 h post-application are shown in Figure 3.

At 12 and 24 h post-application, the NCs (pH 6) group scores were significantly higher scores than those of the AC (pH 6) and NON groups ($p < 0.05$). In contrast, the NCs (pH 3) group scores were significantly lower than that of the NON group 24 h post-application ($p < 0.05$). At 4 h post-application, scores for the NFs (pH 6) group were significantly higher than those of the AC (pH 6) and NON groups ($p < 0.01$). The GlcNAc group scores were significantly higher 12 h post-application compared to those of the DW group ($p < 0.01$).

3.2. Experiment 2: Effect of NFs on skin cytokine production using Franz cells

The cumulative secreted cytokine concentration in the supernatant (PBS) from each experimental group is shown in Figure 4.

For both IL-1α and TGF-β, the cytokine production increased in the following order: NFs < NCs < DW < AC. The TGF-β levels differed significantly between the NFs and AC groups ($p < 0.01$), and the NCs and AC groups ($p < 0.05$).

4. Discussion

4.1. Experiment 1: The effect of chitin NFs on epithelial cells in a three-dimensional skin culture model

The skin, which is responsible for protecting various internal organs from the external environment, is composed of the epithelium and the corium and is supported by subcutaneous tissues. The epithelium consists of the cornified layer (CL), granular layer (GL), spinosum layer (SL), and basal layer (BL). Of the skin layers, the CL is responsible for acting as a protective barrier, and hence is an important part of the epithelium as it protects the internal structures from desiccation or against changes in the environment, while maintaining appropriate hydration for function within the environment, for example, UV, desiccation and chemical substances. [15]. Secretions from the sebaceous glands that cover the outermost layer, secretions from granule cells, and keratinocytes participate in CL formation. Intercellular lipids and natural moisturizing factors (NMF) are composed of secretions from granule cells in the CL, and facilitate the barrier and moisturizing functions. NMFs are complex mixtures of lactic acid, urea, citrate, sugars, and amino acids such as pyrrolidone carboxylic acid (PCA), urocanic acid and its derivatives [16]. Intercellular lipids regulate moisture evaporation from the skin, but this phenomenon is known to decrease with age. In senile xerosis, a reduction in the number of keratohyalin granules has been observed [17], and there are reports that the granule cells and lamellar body numbers increase in hairless mice grown under dry environments [18]. The essential role that NMFs play in the moisturizing and barrier functions of skin underscores the critical function of the granular layer and the associated granules, as they are

responsible for secretion of both lipids and NMFs. Additionally, it has been reported that tight junctions in the second uppermost layer (SG2) of the granular layer seal intercellular gaps [19].

Our current study reveals that even if topical treatments are not directly applied to the CL, the maintenance of proper culture and moisturizing conditions below the epithelium leads to favorable granular layer development, with an increase in granule density. However, if skin cells were cultured without the application of substances to the CL, low intercellular gap and nucleus clarity scores were obtained and maintenance of cellular integrity was not possible. Similar to previous studies, our current report suggests that the granule cell number is increased as a defense mechanism upon disruption of cellular integrity.

As shown in Figures 2A and 2C, both the NFs (pH 6) and NCs (pH 6) group scores were favorable compared to those of their respective controls or the NON group, at all measured time points. Application of NFs (pH 6) or NCs (pH 6) appears result in tighter intercellular spacing and promotes the maintenance of cellular integrity, when compared to non-treated cells.

These results suggest that the application of chitin NFs to skin protects epithelial cells. Although the precise mechanism remains unknown, this effect may be attributable to its ability to prevent moisture evaporation. Moreover, as shown in Figures 2A and 2B, the NCs (pH 6) group scored higher on measured criteria compared to the NFs (pH 6) group at all time points after the first 8 h of application, indicating that NCs is the more effective skin protector in the long-term. In contrast, as shown in Figures 2B and 2D, the scores for NFs (pH 3) and NCs (pH 3) decreased compared to those of the control or NON groups, beginning at 12 h

post-application. This suggests that pH is an important criterion for topical formulations, and that pH 6 is more effective than pH 3 for epithelial cell protection.

In the GlcNAc group, the granular layer score fell below 2.5 points by 24 h post-application. At this time, the granule cell density and intercellular gap scores were 1.0 and 0.6 points, respectively. Histological images 24 h post-application revealed a granular layer that had nearly disappeared or was 1-layer thick in some portions of the image. As stated above, granule cells secrete substances that constitute the CL, thereby conferring its barrier function. Furthermore, there are tight junctions in the SG2 layer of the granular layer, which in combination with the granule density and number of layers within the cell, are likely important for its barrier function. The granular layer score 24 h post-application for the GlcNAc group was 2.1 points, which is lower than that of the NFs (pH 6) and NCs (pH 6) groups. In addition, the granule density was lower in the GlcNAc group than the NFs (pH 6) and NCs (pH 6) groups. This suggests that the application of GlcNAc to the skin does not contribute to long-term skin cell protection. In contrast, 24 h post-application histological images of the NFs and NCs group samples showed that at least 2 layers of the granular layer were maintained and that many granules were present. All of these observations indicate that the application of NFs (pH 6) and NCs (pH 6) contributes more significantly to epithelial cell protection than does application of GlcNAc.

4.2. Experiment 2: Effect of NFs on skin cytokine production using Franz cells

Keratinocytes in skin produce a high level of IL-1α, and activated IL-1α is abundant in the cuticle [20]. Furthermore, molecules isolated from house dust

mites have been shown to induce pro-inflammatory cytokine and chemokine release from epidermal keratinocytes and skin fibroblasts [21], there are many environmental stimuli that can be inflammatory. The cytokine TGF-β is secreted from T-cells and functions as an immunosuppressive factor. TGF-β regulates immune cell differentiation, proliferation, activation, and can contribute to pathologies such as cancer, autoimmunity, and opportunistic infection [22]. TGF-β is a suppressive factor that regulates wound and skin-inflammation-related cellular processes [23].

In mouse hepatocytes, TGF-β suppresses the IL-1α-induced expression of IL-1R as well as TLR2 [24]. Patients with osteomyelofibrosis have activated NF-κB due to monocyte adhesion, leading to IL-1 production, which in turn stimulates TGF-β production and causes bone marrow fibrosis [25]. Based on these interactions, inflammatory cytokines such as IL-1α and suppressive cytokines such as TGF-β are intimately related. Findings from a *Nocardia brasiliensis*-induced mouse footpad immunoreactivity model showed that both inflammatory- and anti-inflammatory cytokines are produced simultaneously by host cells [26]. Taken together, the involvement of IL-1 in TGF-β production can be explained through a similar model, whereby production of TGF-β is intricately linked to the production of IL-1.

In our current study, the sum of cytokine concentrations at each time point was considered as the cumulative cytokine production level. The cumulative cytokine production level in the NFs and NCs groups was lower than that in the AC and DW groups. Although a significant difference in the IL-1 production in the NFs/NCs and AC/DW groups was not observed, a significant difference in TGF-

β production was detected. TGF-β production in the NFs (pH 6) group was lower than that in the NCs (pH 6) group. On the other hand, the NCs (pH 6) group scored was higher on measured criteria compared to the NFs (pH 6) group in experiment 1. These experiments revealed that NFs and NCs protected skin cells. The reason of the difference in effects for skin protect between the two materials was still unclear. One of the mechanisms was considered that 3D structure of NFs and NCs contained water and prevent from skin dryness. In future, it needs further research to verify mechanisms of reduction of inflammatory cytokine when NFs and NCs were applied to skin.

5. Conclusions

The results of our study suggested that NFs and NCs protect skin cells while being less inflammatory. Further research is necessary to determine precisely how NFs and NCs can be incorporated into the manufacture of cosmetics or textiles.

References

[1] P. Y. Chen, A. Y. Lin, J. McKittrick, and M. A. Meyers, Structure and mechanical properties of crab exoskeletons. *Acta Biomaterialia*, 4, 587–596. (2008).

[2] D. Raabe, P. Romano, C. Sachs, H. Fabritius, A. A. Sawalmih, S. B. Yi, G. Servos, and H. G. Hartwig, Microstructure and crystallographic texture

of the chitin–protein network in the biological composite material of the exoskeleton of the lobster Homarus americanus. *Materials Science and Engineering A*, 421, 143–153. (2006).

[3] S. Nikolov, H. Fabritius, M. Petrov, M. Friak, L. Lymperakis, C. Sachs, D. Raabe, and J. Neugebauer, Robustness and optimal use of design principles of arthropod exoskeletons studied by ab initio based multiscale simulations. *Journal of The Mechanical Behavior of Biomedical Materials*, 4, 129-145. (2011).

[4] H. O. Fabritius, E. S. Karsten, K. Balasundaram, S. Hild, K. Huemer, and D. Raabe, Correlation of structure, composition and local mechanical properties in the dorsal carapace of the edible crab *Cancer pagurus*. Zeitschrift fur Kristallographie, 227 (11):766-776; 10.1524/zkri.2012.1532. (2012).

[5] R. A. A. Muzzarelli, P. Morganti, G. Morganti, P. Palombo, M. Palombo, G. Biagini, M. M. Belmonte, F. Giantomassi, F. Orlandi, and C. Muzzarelli, Chitin nanofibrils/chitosan glycolate composites as wound medicaments. *Carbohydrate Polymers*, 70, 274–284. (2007).

[6] N. K. Gopalan and A. Dufresne, Crab shell chitin whisker reinforced 318 natural rubber nanocomposites 1. Processing and swelling behavior. *Biomacromolecules,* 4, 657–665. (2003).

[7] J. F. Revol and R. H. Marchessault, In vitro chiral nematic ordering of chitin crystallites. *International Journal of Biological Macromolecules*, 15, 329–335. (1993).

[8] Y. Fan, T. Saito, and A. Isogai, Preparation of chitin nanofibers from squid pen beta-chitin by simple mechanical treatment under acid conditions. *Biomacromolecules*, 9, 1919-1923. (2008).

[9] S. Ifuku and H. Saimoto, Chitin nanofibers: preparations, modifications, and applications. *Nanoscale*, 4, 3308–3318. (2012).

[10] R. A. A. Muzzarelli, Chitins and chitosans for the repair of wounded skin, nerve, cartilage and bone. *Carbohydrate Polymers*, 76 167-182. (2009).

[11] R. A. A. Muzzarelli, Chitins and chitosans as immunoadjuvants and non-allergenic drug carriers. *Marine Drugs*, 8, 292-312. (2010).

[12] K. Azuma, T. Osaki, T. Wakuda, S. Ifuku, H. Saimoto, T. Tsuka, T. Imagawa, Y. Okamoto, and S. Minami, Beneficial and preventive effect of chitin nanofibrils in a dextran sulfate sodium-induced acute ulcerative colitis model. *Carbohydrate Polymers*, 87, 1399–1403. (2012).

[13] S. Ifuku, M. Nogi, M. Yoshioka, M. Morimoto, H. Yano, and H. Saimoto, Fibrillation of dried chitin into 10–20 nm nanofibers by a simple grinding method

under acidic conditions Carbohydrate Polymers, 81, 134-139. (2010).

[14] S. Minami and Y. Okamoto, Tottori University, Drug for the treatment of the wound, Japan patent, 4,496,375. April 23. (2010).

[15] A. W. Rawlings and C. R. Harding. Moisturization and skin barrier function. *Dermatologic Therapy* 17, 43–48. (2004).

[16] E. J. Cler and A. Fourtanier, L'acide pyrrolidone carboxylique (PCA) et la peau. *International Journal of Cosmetic Science*, 3, 101–113. (1981).

[17] T. Tezuka, Electron-microscopic changes in xerosis senilis epidermis. Its abnormal membrane-coating formation. *Dermatologica*, 166, 57–61. (1983).

[18] M. Denda, J. Sato, Y. Masuda, T. Tsuchiya, J. Koyama, M. Kuramoto, P. M. Elias, and K. R. Feingold, Exposure to a dry environment enhances epidermal permeability barrier function. *Journal of Investigative Dermatology*, 111, 858–863. (1998).

[19] A. Kubo, K. Nagao, M. Yokouchi, H. Sasaki, and M. Amagai, External antigen uptake by Langerhans cells with reorganization of epidermal tight junction barriers. *Journal of Experimental Medicine*, 13, 2937–2946. (2009).

[20] S. Kezic, G. M. O'Regan, R. Lutter, I. Jakasa, E. S. Koster, S. Saunders,

P. M. Caspers, J. H. Kemperman, G. J. Puppels, A. Sandilands, H. Chen, L. E. Campbell, K. Kroboth, R. Watson, P. G. Fallon, W. H. I. McLean, and A. D. Irvine, Filaggrin loss-of-function mutations are associated with enhanced expression of IL-1 cytokines in the stratum corneum of patients with atopic dermatitis and in a murine model of filaggrin deficiency. *Journal of Allergy and Clinical Immunology*, 4, 1031–1039. (2012).

[21] L. G. Arlian and M. S. Morgan, Immunomodulation of skin cytokine secretion by house dust mite extracts. *International Archives of Allergy and Immunology,* 156, 171–178. (2011).

[22] J. J. Letterio and A. B. Roberts, Regulation of immune responses by TGFβ. *Annual Review of Immunology*, 16, 137–161. (1998).

[23] M. Anthoni, G. Wang, C. Deng, H. J. Wolff, A. I. Lauerma, and H. T. Alenius, Smad3 signal transducer regulates skin inflammation and specific IgE response in murine model of atopic dermatitis. *Journal of Investigative Dermatology*, 127, 1923–1929. (2007).

[24] T. Matsumura, H. Hayashi, T. Takii, C. F. Thorn, W. S. Whitehead, J. I. Inoue, and K. Onozaki, TGF-β down-regulates IL-1α induced TLR2 expression in murine hepatocytes. *Journal of Leukocyte Biology,* 75, 1056–1061. (2004).

[25] P. Rameshwar, R. Narayanan, J. Qian, T. N. Denny, C. Colon, and P.

Gasco´n, NF-kB as a central mediator in the induction of TGF-b in monocytes from patients with idiopathic myelofibrosis: an inflammatory response beyond the realm of homeostasis. *Journal of Immunology*, 165, 2271–2277. (2000).

[26] J. M. Solis-Soto, L. E. Quintanilla-Rodriguez, I. Meester, J. C. Segoviano Ramirez, J. L. Vazquez-Juarez, and M. C. Salinas Carmona, In situ detection and distribution of inflammatory cytokines during the course of infection with Nocardia brasiliensis. *Histology and Histopathology*, 23, 573–81. (2008).

Figures and tables

Table 1. The results of histological scoring in each group

		nucleus clearly	intercellular gap	granule density	number of the granule layers	Total (mean ± SE)
NON	4 h	0.81	0.84	2.19	2.94	6.78 ± 0.51
	12 h	0.34	0.34	2.19	3.13	6.00 ± 0.32
	24 h	0.38	0.25	1.88	3.09	5.59 ± 0.19
DW	4 h	0.71	0.56	1.92	3.08	6.27 ± 0.23
	12 h	0.75	0.63	1.60	2.42	5.40 ± 0.35
	24 h	0.73	0.21	1.15	2.10	4.19 ± 0.38
Ac (pH3)	4 h	1.00	1.44	1.75	2.84	7.03 ± 0.18
	12 h	1.00	1.00	1.34	2.50	5.84 ± 0.34
	24 h	0.94	1.13	1.06	1.75	4.88 ± 0.44
Ac (pH6)	4 h	0.84	1.00	2.16	3.03	7.03 ± 0.21
	12 h	0.69	0.97	1.75	2.63	6.03 ± 0.27
	24 h	0.91	0.66	1.53	2.31	5.41 ± 0.31
NFs (pH3)	4 h	0.97	1.84	1.91	2.69	7.41 ± 0.41
	12 h	1.00	1.28	1.34	2.28	5.91 ± 0.30
	24 h	0.97	1.56	0.84	1.75	5.13 ± 0.37
NFs (pH6)	4 h	0.92	1.33	2.54	3.63	8.42 ± 0.18
	12 h	0.96	1.06	1.90	2.69	6.60 ± 0.17
	24 h	0.94	1.04	1.73	2.65	6.35 ± 0.30
NCs (pH3)	4 h	1.00	1.06	1.81	2.84	6.72 ± 0.30
	12 h	1.00	1.06	1.16	2.00	5.22 ± 0.33
	24 h	0.97	1.00	0.47	1.28	3.72 ± 0.30
NCs (pH6)	4 h	0.88	1.40	2.13	3.23	7.63 ± 0.20
	12 h	0.98	1.35	2.06	3.19	7.58 ± 0.29
	24 h	0.96	1.90	1.67	2.58	7.10 ± 0.20
GlcNAc	4 h	0.77	1.29	2.06	3.10	7.23 ± 0.33
	12 h	0.94	1.27	2.17	2.69	7.06 ± 0.33
	24 h	0.81	0.65	1.00	2.15	4.60 ± 0.21

Intercellular gap scores were consistently low in the no application (NON) and distilled water (DW) groups. The acetic acid (AC) (pH 3) and nanofibrils (NFs) (pH 3) group scores decreased over time. The AC (pH 6) and nanocrystals (NCs) (pH 3) group scores decreased gradually over time. Although scores for the NFs (pH 6) group decreased gradually over time, scores at the 4-h time point were higher compared to those of the other groups, and the scores at the 24-h time point were higher than that of the control groups. Scores for the NCs (pH 6) group remained high over all measured periods. Scores in the N-acetyl-D-glucosamine (GlcNAc) group were high until the 12-h time point but decreased by the 24-h time point.

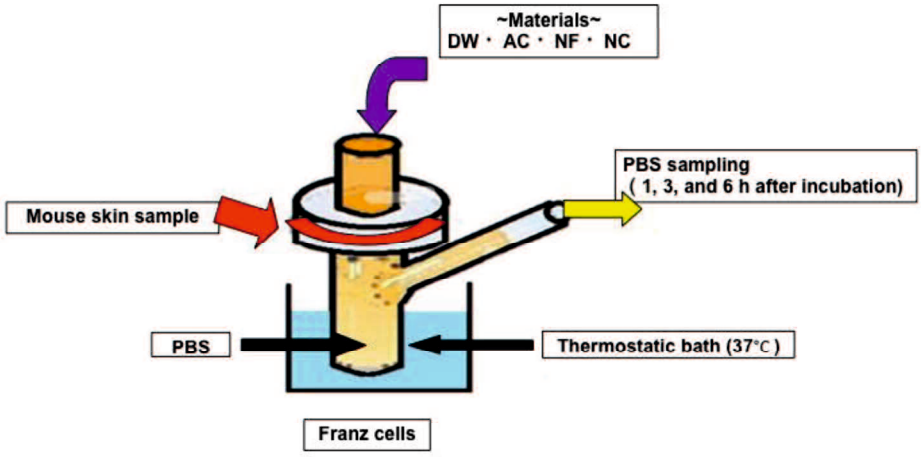

Figure 1. Schematic of the protocol for Experiment 2.

Skin samples were applied to PBS-soaked Franz cells. The samples were incubated in a thermostat chamber for 1 h. Each test material was then applied and the samples were re-incubated. At 1, 3, and 6 h post-application, PBS was aspirated from the cells.

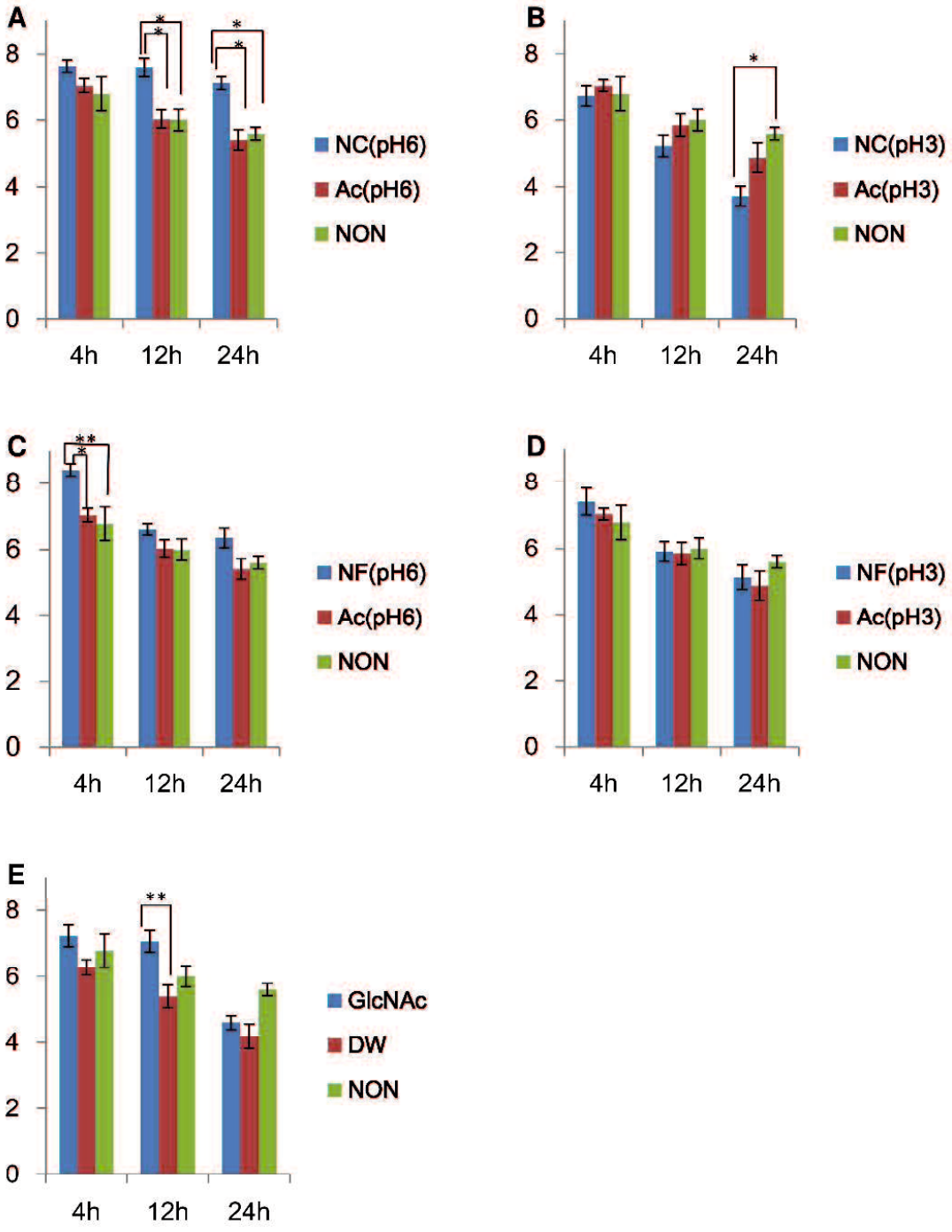

Figure 2. Comparison of the results of histological scoring in each group

(*y*-axis, total scores; *x*-axis, incubation time)

A: Comparison of the nanocrystals (NCs) (pH 6) group and the corresponding

control groups, acetic acid (AC) (pH 6) and no application (NON)

B: Comparison of the nanocrystals (NCs) (pH 3) group and the corresponding control groups, AC (pH 3) and NON

C: Comparison of the NFs (pH 6) group and the corresponding control groups, AC (pH 6) and NON

D: Comparison of the NFs (pH 3) group and the corresponding control groups, AC (pH 3) and NON

E: Comparison of the N-acetyl-D-glucosamine (GlcNAc) group and the corresponding control groups, distilled water (DW) and NON

In the NCs (pH 6) group, scores were significantly higher compared to those in the AC (pH 6) and NON groups 12 and 24 h post-application. In the NCs (pH 3) group, scores were significantly higher compared to those in the NON group 24 h post-application. In the NFs (pH 6) group, scores were significantly higher compared to those in AC (pH 6) and NON groups 4 h post-application. In the GlcNAc group, scores were significantly higher compared to those in the DW group 12 h post-application. The error bars indicate mean ± SE. Significantly different from the AC group (**$P < 0.01$; *$P < 0.05$).

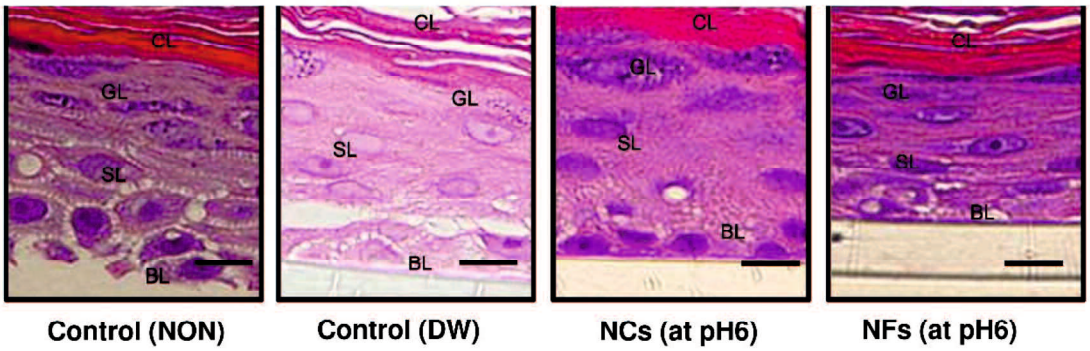

Figure 3. The effect of chitin nanofibrils (NFs) on the EPI-MODEL after 24 h of incubation

The number of layers and granule density were assessed in the granular layer (GL). Intercellular gaps and nucleus clarity were assessed in the spinosum layer (SL). Characteristic observations included large intercellular gaps in the no application (NON) group, low granule density in the distilled water (DW) group and high granule density in the nanocrystals (NCs) (pH 6) and NFs (pH 6) group. (bar = 100 μm)

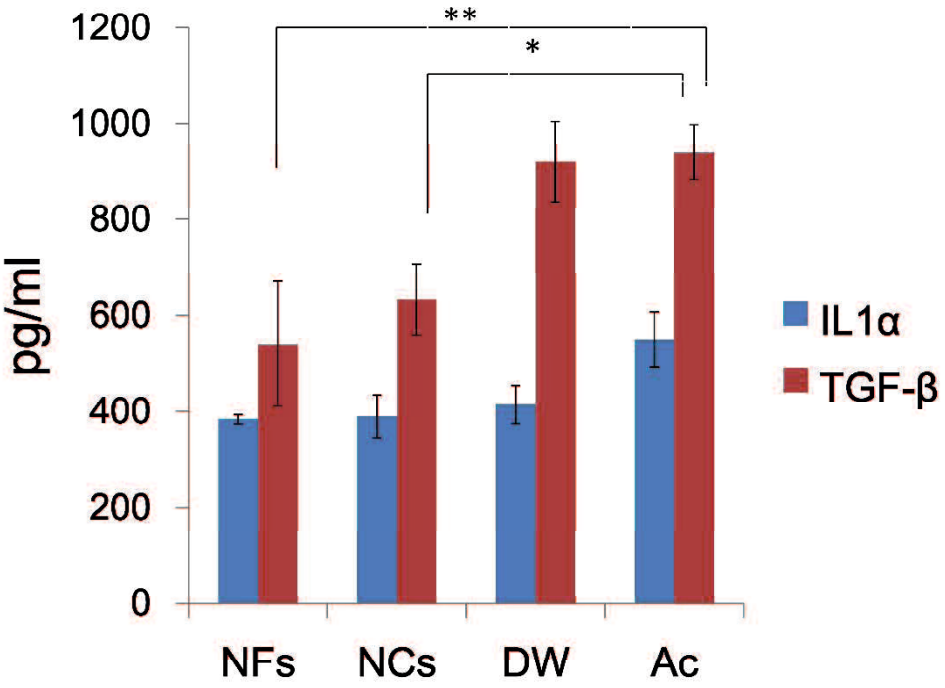

Figure 4. Estimated production of cytokines in each group

For both IL-1α and TGF-β, the cumulative cytokine production increased in the following order: nanofibrils (NFs) < nanocrystals (NCs) < distilled water (DW) < acetic acid (AC). A highly significant difference was confirmed between the NFs and DW groups (IL-1α and TGF-β) and the NFs and AC groups (for TGF-β), whereas a significant difference was confirmed between the NCs and AC groups (IL-1α and TGF-β). The error bars indicate mean ± SE. Significantly different from the AC group (**P <0.01; *P<0.05).

Chapter Ⅱ.

Protective effect of chitin urocanate nanofibers against ultraviolet radiation

Abstract

Urocanic acid (UCA) is a major ultraviolet (UV)-absorbing chromophore. Chitins are highly crystalline structures that are found predominantly in crustacean shells. Alpha-chitin consists of microfibers that contain nanofibrils (NFs) embedded in a protein matrix. Acid hydrolysis is a common method used to prepare chitin NFs. We typically obtain NFs by hydrolyzing chitin with acetic acid. However, in the present study, we used UCA to prepare UCA chitin NFs (UNFs) and examined its protective effect against UVB radiation. Hos:HR-1 mice coated with UNFs were UVB irradiated (302 nm, 150 mJ/cm^2), and these mice showed markedly lower UVB radiation-induced cutaneous erythema than the control. Additionally, sunburn cells were rarely detected in the epidermis of UNFs-coated mice after UVB irradiation. Although the difference was not as significant as UNFs, the number of sunburn cells in mice treated with acetic acid chitin NFs (ANFs) tended to be lower than in control mice. These results demonstrate that ANFs have a protective effect against UVB and suggest that the anti-inflammatory and antioxidant effects of NFs influence the protective effect of ANFs against UVB radiation. The combination of NFs with other substances that possess UV-protective effects, such as UCA, may provide an enhanced protective effect against UVB radiation.

1. Introduction

1.1. DNA Damage and Skin Damage by UV Light

Ultraviolet (UV) radiation has a harmful effect on the human body. UV radiation can be classified according to wavelength as UVA (320–380 nm), UVB (290–320 nm), and UVC (210–290 nm). Because the ozone layer blocks UVC radiation, only UVA and UVB reach the earth's surface. UV radiation with shorter wavelengths has higher energy and is more likely to cause skin damage. Exposure to UVB causes DNA damage and dermatopathies such as inflammation, pigmentation, skin aging, photoallergy, skin cancer, and immune dysfunction [1, 2]. The mechanism underlying DNA damage has been determined as follows: DNA has a maximum absorption at approximately 260 nm; therefore, UVC and some UVB radiation of certain wavelengths can cause DNA nucleotides to absorb energy, which results in their transition to an excited state. Molecules in such an excited state are unstable, and in order for them to return to a stable state, new chemical bonds are formed. These differ from the original bonds, and this shift damages the DNA [1]. In addition, DNA damage also occurs as a result of irradiation with UVA or UVB rays within a range of wavelengths where there is no UV absorption. This is thought to be due to reactive oxygen species (ROS), which are generated as a result of irradiation [3]. Chromophores such as NADH and FAD, which absorb UV rays, are present in the cell and are activated by light energy. As a result, ROS, such as O2-, H_2O_2, and $^1O_2$, are generated from oxygen. These ROS cause lipid peroxidation, protein polymerization or cleavage, enzyme deactivation, and various types of DNA damage. The potential DNA damage includes the production of thymine glycol due to thymine peroxidation as well as

the production of uracil due to cytosine deamination [1]. In addition, ROS attack adenine and guanine, which causes cleavage of the imidazole ring and oxidation of guanine. DNA strands can also break. Such DNA damage is difficult to repair [1].

UVB-induced cutaneous damage leads to erythema, one of the cardinal signs of inflammation. Non-steroidal anti-inflammatory drugs (NSAIDs) suppress the early stages of erythema very well; however, their suppressive efficacy gradually weakens after the initial stage, regardless of whether or not the skin is treated with additional NSAIDs. It has been suggested that prostaglandins (PGs) might be responsible for the early phase of erythema that is depressed by NSAIDs; however, other factors may be involved in prolonging the duration of erythema [4]. Sunburn begins several h after exposure, and flaring of the skin, swelling, and bullous formation peak 12–24 h later [1]. In the present study, the skin was observed for up to 24 h after exposure, when erythema peaks.

One in five Americans suffers from skin cancer [5], for which UV irradiation is the primary cause [6]. Risk of skin cancer is influenced by UV irradiation and skin pigmentation [7]. Hence, UV ray-blocking experiments using UVB irradiation have been performed by many scientists. Yasuoka et al. irradiated the back skin of hairless mice with 5 kJ/m^2 UVB irradiation [8], and Mizukoshi et al. used 100 mJ/cm^2 UVB irradiation to evaluate irradiation blocking ability [9]. By those various experiments, various sun protection materials are widely manufactured and used. The proof of these materials' efficacy is of great significance for the protection of public health, as the UVB rays of solar radiation are the main contributors to sunburn, immunosuppression, and skin cancer [10]. According to

Ananthaswamy et al., application of SPF-15 sunscreen to mouse skin before each UV irradiation nearly eliminated p53 mutations, which play an essential role in skin cancer development [11].

In recent years, the demand for new, more functional sun protection materials has increased as the risk of the UV exposure has risen due to depletion of the ozone layer.

1.2. About UCA and Squid Ink as Positive Controls

The breakdown of filaggrin into hygroscopic free amino acids and their derivatives is the major contributor to the natural moisturizing factor (NMF) that is produced within the stratum corneum [12]. NMF is responsible for maintaining skin hydration and water retention within the stratum corneum under conditions of low environmental humidity [12]. Filaggrin is particularly rich in histidine. Histidine is deiminated into trans-UCA (*trans*-UCA) by the catalytic action of histidase, and presumably provides a major source of epidermal UCA [13, 14].

UCA is an intermediate metabolite of histidine and is present mainly in the stratum corneum. UCA is a major UV-absorbing chromophore in the skin [15]. *Trans*-UCA is a major UVR-absorbing skin molecule that undergoes a photoisomerization to its *cis*-isomer following UVR exposure. Cis-UCA has been shown to have immunosuppressive properties, whereas trans-UCA may act as a natural sunscreen due to its UV-absorbing properties [16]. *Trans*-UCA has also been reported to inhibit UVB-induced secretion of IL-6 and IL-8 in the cornea [17], and it is an important protective factor against UV radiation.

Squid ink is comprised of eumelanin, a well-known natural UV ray absorber. The

beneficial effects of melanin are mainly due to the presence of eumelanin, which scatters and absorbs 50–75% of UVR. Eumelanin also scavenges UV-generated free radicals, which protect against UVR damage in deeper layers [18]. Therefore, we decided to use squid ink as a positive control.

1.3 About Chitin and Chitin Nanofibers

Chitins are highly crystalline structures that are found predominantly in crustacean exoskeletons, insects, cuttlefishes, shellfishes, mushrooms, and fungi. Alpha-chitin is composed of microfibers that are comprised of NFs, which are approximately 2–5 nm in diameter and 30 nm in length and embedded in a protein matrix [19,20]. Isolated chitin NFs have potential for use in drug delivery systems, tissue-engineering scaffolds, and wound dressings [21]. We have recently succeeded in isolating alpha-chitin NFs from crab shells by a simple process [22]. An acidic condition is key to fibrillating the chitin effectively. A small number of amino groups in the chitin are cationized by the addition of an acid, which promotes the fibrillation of chitin into nanofibers by electrostatic repulsion.

NFs are thought to have great potential for various applications because they have several useful properties, including high specific surface area and high porosity [23, 24]. Many studies have demonstrated the potential applications of chitin and chitosan NFs in tissue engineering, as wound dressings, in cosmetic and skin products, in stem cell technology, as anti-cancer treatments, as drug delivery systems, and as treatments for obesity and inflammatory conditions [25]. Until now, we have obtained NFs by hydrolyzing chitin with acetic acid.

In this study, we prepared UCA chitin NFs (UNFs) by UCA hydrolysis. We

hypothesized that we could generate valuable new NFs with UV-blocking function by preparing NFs with UCA, and we examined the protective effect of the UNF against UV radiation.

2. Materials and methods

2.1. Test Specimens

As shown in Table 1, mice were divided into seven experimental groups and treated with the following substances: (1) Acetic acid (Ac) cream (1 wt% Ac aqueous solution mixed with hydrophilic ointment [HO; NIPRO Pharma Corporation Co., Ltd., Osaka, Japan] at a ratio of 1:1); (2) HO (HO only); (3) Polyethylene glycol (PG) cream (35 wt% PG aqueous solution [NOF Corporation, Tokyo, Japan] mixed with HO at a ratio of 1:1); (4) Acetic acid chitin nanofibrils (ANFs) cream (0.82 wt% ANFs and 99.18 wt% [1 wt% Ac] aqueous solution mixed with HO at a ratio of 1:1); (5) UCA cream (0.2 wt% UCA and 35 wt% PG as an aqueous solution mixed with HO at a ratio of 1:1); (6) UNFs cream (1 wt% UNFs and 99 wt% [0.2 wt% UCA and 30 wt% PG] as an aqueous solution mixed with HO at a ratio of 1:1); (7) Squid ink (SI) cream (1 wt% SI and 35 wt% PG in an aqueous solution mixed with HO at a ratio of 1:1).(Table 1)

Acetic acid (Ac) cream: 1 wt% Ac aqueous solution mixed with hydrophilic ointment (HO) at a ratio of 1:1; HO: HO only; Polyethylene glycol (PG) cream: 35 wt% PG aqueous solution mixed with HO at a ratio of 1:1; Acetic acid chitin nanofibrils (ANFs) cream: 0.82 wt% ANFs and 99.18 wt% (1 wt% Ac) as an aqueous solution mixed with HO at a ratio of 1:1; UCA cream: 0.2 wt% UCA and 35 wt% PG as an aqueous solution mixed with HO at a ratio of 1:1; UNFs cream:

1 wt% UNFs and 99 wt% (0.2 wt% UCA and 30 wt% PG) as an aqueous solution mixed with HO at a ratio of 1:1; Squid ink (SI) cream: 1 wt% SI and 35 wt% PG in an aqueous solution mixed with HO at a ratio of 1:1.

The samples were prepared according to the following methods: Ac cream was prepared in distilled water at a final concentration of 1 wt%. Next, 1 mL of the aqueous solution was mixed with 1 g of HO. To prepare the PG cream, an aqueous solution of PG was prepared by mixing 84 g of an aqueous solution of 40 wt% PG (molecular weight 20,000) with 12 g of distilled water. Then 1 mL of the aqueous solution was mixed with 1 g of HO. To prepare the ANFs cream, 197 g of purified water was added to 2 g of crab shell-derived chitin powder (Nacalai Tesque, Inc., Kyoto, Japan, deacetylation degree: <5%) and stirred overnight. The aqueous solution was subjected to 30 passes on a Star Burst system (Star Burst Mini, HJP-25001S; Sugino Machine Co., Ltd. Toyama, Japan) at 245 MPa. Finally, 1 mL of the aqueous solution was mixed with 1 g of HO. To prepare the UCA cream, a PG aqueous solution was prepared by mixing 84 g of an aqueous solution of 40 wt% PG with 12 g of distilled water. Next, 0.192 g of UCA (Sigma-Aldrich, USA) was added to the aqueous solution and stirred until it dissolved. Finally, 1 mL of the aqueous solution was mixed with 1 g of HO. To prepare the UNFs cream, 2 g of UCA was added to 1 L of distilled water and dissolved by heating at 40°C. Ten grams of crab shell-derived chitin powder was added to the UCA aqueous solution, and the mixture was used as a chitin suspension. The suspension was defibrated twice using a millstone grinder (MKCA6-3; Masuko Sangyo Co., Ltd., Saitama) at 1,500 rpm. An aqueous solution of 30 wt% PG was added to this sample. Then 1 mL of the aqueous solution was mixed with 1 g of

HO. To prepare the SI cream, 60 g of distilled water was added to 40 g of PG, and the mixture was dissolved to obtain an aqueous solution of 40 wt% PG. Next, 12 g of ikasumi melamine (melanin density 8 wt%) was added to 84 g of an aqueous solution of 40 wt% PG and stirred. The aqueous solution was adjusted so that it would contain 1 wt% ikasumi melamine and 35 wt% PG. Finally, 1 mL of the aqueous solution was mixed with 1 g of HO. The UCA contained trans-UCA.

2.2. Experimental Animal Model

Male 8–9-week-old Hos:HR-1 mice (25–35 g, Hoshino Laboratory Animals Inc., Ibaraki, Japan) were used. All animal care and experimentation procedures were approved by the Animal Research Committee of Tottori University.

2.3. Experimental Groups

The mice were divided into nine groups: The Ac cream group (n = 5), HO (n = 5), PG cream (n = 5), ANFs cream (n = 5), UCA cream (n = 5), UNFs cream (n = 5), SI cream (n = 5), C (+) (non-coated, irradiated; n = 5), and C (-) (non-coated, non-irradiated; n = 5) groups.

2.4. Sample Application and UV Irradiation

Each sample (2 g) was applied to the left side of the back of the test mice. In addition to the seven sample groups, two control groups were included in this study. In one group, no sample was applied to the mice, but they were irradiated [the positive control, C (+)], and in another group, no sample was applied and the

mice were not irradiated [C (-)]. All of the groups were irradiated (150 mJ/cm^2) with a UV crosslinker (Model CL-1000M, 302 nm UV; UVP, USA). In accordance with the criteria established by the OECD, erythema of the skin was assessed at 2, 4, 6, 12, and 24 h after irradiation.

2.5. Preparation of Irradiated Samples

Twenty-four h after UV irradiation, the animals were euthanized by cervical dislocation, and the skin at the irradiated site was sampled using a Dermapunch (8 mm; Nipro Co., Osaka). The collected skin samples were immersed and fixed in 10% formalin (Mildform 10N; Wako Pure Chemical Industries Ltd., Osaka, Japan). The skin surface samples were cut into 4-μm thick vertical slices for cross-sectional observation. Histological observations were performed after hematoxylin-eosin (H&E) and TUNEL staining.

2.6. Evaluation Methods

The erythema score was determined as the mean score of two observers, in accordance with OECD standards, at 2, 4, 6, 12, and 24 h after UV irradiation at the site of sample application. The presence of sunburn cells in the epidermis was evaluated using specimens prepared by TUNEL staining. Basal cells (n = 100) inside the epidermis were counted (excluding hair follicle cells), and the number of TUNEL-positive sunburn cells present between granular cells was counted. These measurements were conducted at four random times, and the mean number of sunburn cells per 100 cells was recorded.

2.7. Statistical Analysis

Data analysis was performed using 4-step Excel Statistics (OMS Publishing, Saitama, Japan). For each experiment, we performed Bartlett's test for normality. For those where we confirmed normality or equal variance, single-factor ANOVA was performed; otherwise, we used the Kruskal-Wallis test. Afterwards, a multiple comparison test (Tukey-Kramer test or Scheffé's F-test) was performed. *P* values less than 0.05 were considered statistically significant, and *P* values less than 0.01 were considered highly significant.

3. Results and Discussion

3.1. Erythema Score

All of the groups were irradiated (150 mJ/cm^2) with UV (302 nm). In accordance with the criteria established by the OECD, erythema of the skin was assessed at 2, 4, 6, 12, and 24 h after irradiation.

As shown in Figure 1, compared to the C (+) group, UV radiation-induced erythema was markedly reduced in the SI cream group. The erythema score for the C (+) group was similar to the erythema scores for the HO, PG cream, Ac cream, and ANFs cream groups. In addition, compared with the C (+) group, UV irradiation-induced erythema was markedly inhibited in the UNFs cream group as compared to the Si cream group, which was the positive control. Erythema in the UCA cream group was mildly inhibited.

In Figure 2, the degree of erythema in each group is shown as a score. Two h after UV irradiation, the erythema scores for the UNFs cream and SI cream groups were significantly lower than those of the C (+), HO, PG cream, Ac cream,

and ANFs cream groups. The erythema scores for the UCA cream group were significantly lower than those of the C (+), HO, PG cream, and Ac cream groups.

Four h after UV irradiation, the erythema score for the UNFs cream group was significantly lower than the scores for the C (+), HO, PG cream, Ac cream, and ANFs cream groups. The erythema scores for the UCA cream and SI cream groups were significantly lower than those of the C (+), HO, PG, and Ac groups.

Six h after UV irradiation, the erythema score for the UNFs group was significantly lower than those of the C (+), HO cream, PG cream, Ac cream, ANFs cream, and UCA cream groups. The erythema score for the SI group was significantly lower than those of the C (+), HO, PG cream, Ac cream, and ANFs cream groups.

Twelve h after UV irradiation, the erythema scores for both the UNFs cream and SI cream groups were significantly lower than those of the C (+), HO, PG cream, Ac cream, and ANFs cream groups.

Twenty-four h after UV irradiation, the erythema score for the UNFs cream group was significantly lower than the scores for the C (+), HO cream, PG cream, Ac cream, and ANFs cream groups. The erythema score for the SI cream group was significantly lower than those of the C (+) and HO groups.

3.2 Sunburn Cell Counts in the Epidermis

Within h after UVB irradiation, the skin shows reddening, swelling, and vesicle formation, which is referred to as a “sunburn.” Apoptosis occurs as a result of DNA fragmentation due to UV irradiation [26–29], and such apoptotic cells are called “sunburn cells.” Sunburn cells are characterized by cytoplasm with

concentrated nuclei and an increase in eosinophilic staining [30].

The presence of sunburn cells in the epidermis was evaluated using specimens prepared by TUNEL staining. TUNEL staining is a technique that facilitates visualization of fragmented DNA by using terminal deoxynucleotidyl transferase and biotinylated deoxyuridine triphosphate [31]. Thus, using TUNEL staining, we identified cells that became apoptotic as a result of UVB irradiation. The number of TUNEL-positive sunburn cells present between granular cells was counted.

Figure 3 shows a picture of H&E-stained cutaneous tissue at 24 h after UV irradiation, and Figure 4 shows the TUNEL staining of the same tissues. In the C (+) group, the boundary between the dermal layer and the basal layer of the epidermis was unclear, and sunburn cells with eosinophilic cytoplasm and aggregated nuclei were observed (Figure 3). The histological findings for the SI cream group were similar to those for the C (-) group: the boundary between the dermal and basal layers of the epidermis was clear, and no sunburn cells were detected. The histological findings for the HO, PG cream, and Ac cream groups were similar to those for the C (+) group, and the presence of sunburn cells was confirmed.

The presence of sunburn cells could not be confirmed in the UCA cream and UNFs cream groups, and the boundary between the dermal and basal layers of the epidermis was clear. In the ANFs cream group, the boundary between the dermal and basal layers of the epidermis was slightly unclear; however, very few sunburn cells could be detected.

In the C (+), HO, PG cream, Ac cream, and ANFs cream groups, TUNEL-positive sunburn cells were observed from the basal layer of the epidermis to the

stratum spinosum (Figure 4). In the C (+) group, sunburn cells were observed in large numbers; however, they were not found in the SI group. Similar numbers of sunburn cells were observed in the HO, PG cream, Ac cream, and ANFs cream groups. Sunburn cells were present in the ANFs cream group; however, they were nearly absent in the UCA cream and UNFs cream groups.

The sunburn cell counts determined from the TUNEL staining are shown in Figure 5. The sunburn cell counts in the UCA, UNFs, SI, and C (-) groups were significantly lower than those of the C (+), HO, PG cream, and Ac cream groups. The sunburn cell counts in the HO, PG cream, Ac cream, and ANFs cream groups were significantly lower than those of the C (+) group.

3.3. Conclusions in These Two Results

In this study, we examined the protective effects of various formulations against UV radiation, with a focus on UV irradiation-induced erythema and sunburn cells. The sunburn cell count results demonstrated that the UNFs cream, UCA cream, and SI cream significantly and equivalently prevented the generation of sunburn cells. The erythema scores showed differences among the UNFs cream, UCA cream, and SI cream groups; however, these differences were not significant. Compared with UCA cream and SI cream, which was used as a positive control, UNFs cream controlled erythema. UNFs cream inhibited erythema more conspicuously than UCA cream. The UCA cream erythema score rose over time, but UNFs cream maintained approximately the same low score from 2 h to 12 h. Thus, the UNFs cream inhibited erythema by UV irradiation better than the UCA cream did. Moreover, although the differences were not significant, we obtained

interesting results with the ANFs cream. ANFs cream controlled the generation of sunburn cells and erythema at 2, 4, and 6 h when compared with the C (+) group, as well as with the HO, PG cream, and Ac cream groups. The results of our previous study suggested that NFs has anti-inflammatory effects. When we measured the levels of secreted cytokines from the skin of HR-1 mice treated with NFs using Franz cells, we noted that there was less IL-1α and TGF-β secreted from NFs-treated samples than from the control [32]. Inflammatory cytokines such as IL-1α induce the expression of COX-2 and increase the number of PGs. It has been suggested that NFs controls the expression of COX-2 by controlling inflammatory cytokines, which suppresses inflammation of the skin and reduces erythema. In addition, various studies have shown the antioxidant effects of chitin. Ngo *et al*. (2008) determined that chitin oligomers released by the acidic hydrolysis of crab chitin had inhibitory effects on myeloperoxidase (MPO) activity in human myeloid cells, and their direct radical scavenging effect and intracellular glutathione levels increased significantly in a time-dependent manner [33]. Azuma et al. (2012) evaluated the anti-inflammatory effects of orally administered NFs in a mouse model of experimental inflammatory bowel disease (IBD). The number of MPO-positive cells in the submucosal layer was significantly lower in the NFs group than in the control group [34]. These results suggest that chitin and NFs act as antioxidants. The results of our study suggest that the antioxidant effect of NFs may reduce DNA damage and ROS production due to UV irradiation and controls the generation of sunburn cells. They also suggest that UNFs is a superior sun protection material to UCA alone.

4. Conclusion

This study demonstrated that UNFs has a protective effect against UVB irradiation and inhibits UVB irradiation-induced erythema and sunburn cell generation. In addition, the results suggested that NFs itself has a protective effect against UVB, and that the anti-inflammatory and antioxidant effects of NFs affect its protective effect against UVB. This study also showed that UNFs has a protective effect against UVB, and inhibits UVB irradiation-induced erythema and sunburn cell generation. Likewise, the results suggested that NFs has a protective effect against UVB, and that the anti-inflammatory and antioxidant effects of NFs may affect its protective effect against UVB. A combination of NFs and UCA might show a greater Anti-UV effect than conventional preparations do. Further studies are needed to elucidate the underlying mechanism, investigate the anti-inflammatory and antioxidant effects of UNFs, and digitize the UV-ray absorbency of UNFs.

References

[1] S. Kobayashi, UVB-induced skin damage and the protection/treatment—effects of a novel, hydrophilic gamma-tocopherol derivative. *Yakugaku Zasshi*, *126*, 677–693. (2006).

[2] E. C. De Fabo and F. P. Noonan, Mechanism of immune suppression by ultraviolet radiation in vivo. I. Evidence for the existence of a unique photoreceptor in skin and its role in photoimmunology. *Journal of Experimental Medicine, 157*, 84–98. (1983).

[3] S. Sugawara and K. Nizy, *Sun Ultraviolet Light and Health*, Shokaboh Press: Tokyo, Japan, (1998).

[4] D. S. Snyder, Effect of topical indomethacin on UVR-induced redness and prostaglandin E levels in sunburned guinea pig skin. *Prostagrandins*, *11,* 631–643. (1976).

[5] M. R. Donaldson and B. M. Coldiron, No end in sight: The skin cancer epidemic continues. *Seminars in Cutaneous Medicine and Surgery*, *30*, 3–5. (2011)

[6] C. C. Boring, T. S. Squires, and Tong, Cancer Statistics. *A Cancer Journal for Clinicians, 42*, 19–38. (1992).

[7] D. L. Narayanan, R. N. Saladi, and J. L. Fox, Ultraviolet radiation and skin cancer. *International Journal of dermatology*, *49*, 978–986. (2010).

[8] S. Yasuoka, J. Takata, Y. Karube, E. Katoh, T. Tsuzuki, J. Kizu, M. Tsuchiya, and S. Kobayashi,Topical application of a novel, water-soluble gamma-tocopherol derivative prevents UV-induced skin damage in mice. *Journal of Photochemistry and Photobiology*, *81*, 908–913. (2005).

[9] K. Mizukoshi, H. Oshima, K. Matsumoto, R. Hirose, andT. Fujita, The effects

of serine palmitoyltransferase inhibitor, ISP-I, on UV-induced barrier disruption in the stratum corneum. *Biological and Pharmaceutical Bulletin*, *33*, (2010).

[10] A. K. Mishra, A. Mishra, and P. Chattopadhyay, Assessment of *In vitro* Sun Protection Factor of *Calendula Officinalis* L. (Asteraceae) Essential Oil Formulation. *Journal of Young Pharmacists*, *4*, 17–21. (2012).

[11] H. N. Ananthaswamy, S. M. Loughlin, P, Cox, R. L. Evans, S. E. Ullrich, and M. L. Kripke, Sunlight and skin cancer: inhibition of p53 mutations in UV-irradiated mouse skin by sunscreens. *Nature Medicine, 3*, 510–514. (1997).

[12] A. V. Rawlings and C. R. Harding, Moisturization and skin barrier function. *Dermatology and Therapy, 17,* 43–*48.* (2004).

[13] H. P. Baden and M. A. Pathak, The metabolism and function of urocanic acid in skin. *Journal of Investigative Dermatology, 48***,** 11–17.(1967).

[14] J. P. Walterscheid, D. X. Nghiem, N. Kazimi N, L. K. Nutt, D. J. McConkey, M. Norval, and S. E. Ullrich, Cis-urocanic acid, a sunlight-induced immunosuppressive factor, activates immune suppression via the 5-HT2A receptor. *Proceedings of the National Academy of Sciences of the United States of America*, *103*, 17420–17425. (2006).

[15] C. Barresi, C. Stremnitzer, V. Mlitz, S. Kezic, A. Kammeyer, M. Ghannadan,

K. Posa-Markaryan, C. Selden, E. Tschachler, and L. Eckhart, Increased sensitivity of histidinemic mice to UVB radiation suggests a crucial role of endogenous urocanic acid in photoprotection. *Journal of Investigative Dermatology, 131*, 188–194. (2011).

[16] F. de Fine Olivarius, H. C. Wulf, J. Crosby, and M. Norval, The sunscreening effect of urocanic acid. *Photodermatology, Photoimmunology and Photomedicine, 12*, 95–99. (1996).

[17] J. Viiri, H. M. Jauhonen, A. Kauppinen, T. Ryhänen, T. Paimela, J. Hyttinen, I. Sorri, J. K. Laihia, L. Leino, and K. Kaarniranta, Cis-urocanic acid suppresses UV-B-induced interleukin-6 and -8 secretion and cytotoxicity in human corneal and conjunctival epithelial cells in vitro. *Molecular Vision*, *15*, 1799–1805. (2009).

[18] M. Brenner and J. V. Hearing, The protective role of melanin against UV damage in human skin. *Journal of Photochemistry and Photobiology, 84,* 539–549. (2008).

[19] P. Y. Chen, A. Y. Lin, J. McKittrick, and M. A. Meyers, Structure and mechanical properties of crab exoskeletons. *Acta Biomaterialia, 4*, 587–596. (2008).

[20] D. Raabe, P. Romano, C. Sachs, H. Fabritius, A. A. Sawalmih, S. B. Yi, G. Servos, and H. G. Hartwig, Microstructure and crystallographic texture of the

chitin–protein network in the biological composite material of the exoskeleton of the lobster Homarus americanus. *Materials Science and Engineering*, *421*, 143–153. (2006).

[21] R. A. Muzzarelli, P. Morganti, G. Morganti, P. Palombo, M. Palombo, G. Biagini, M. M. Belmonte, F. Giantomassi, F. Orlandi, and C. Muzzarelli, Chitin nanofibrils/chitosan glycolate composites as wound medicaments. *Carbohydrate Polymers, 70*, 274–284. (2007).

[22] S. Ifuku, M. Nogi, K. Abe, M. Yoshioka, M. Morimoto, H. Saimoto, and H. Yano, Preparation of chitin nanofibers with a uniform width as alpha-chitin from crab shells. *Biomacromolecules*, *10*, 1584–1588. (2009).

[23] H. S. Nalwa, Handbook of Nanostructured Biomaterials and Their Applications in Nanobiotechnology, *American Scientific Publishers: Los Angeles, CA, USA, Vols. 1–2.* (2005).

[24] H. S. Nalwa, Encyclopedia of Nanoscience and Nanotechnology, *American Scientific Publishers: Los Angeles, CA, USA, Vols. 1–25*. (2004/2011).

[25] K. Azuma, S. Ifuku, T. Osaki, Y. Okamoto, S. Minami, Preparation and biomedical applications of chitin and chitosan nanofibers. *Journal of Biomedical Nanotechnology, 10*, 2891–2920. (2014).

[26] K. S. Kane, and E. V. Maytin, Ultraviolet B-induced apoptosis of keratinocytes in murine skin is reduced by mild local hyperthermia. *Journal of Investigative Dermatology, 104*, 62–67. (1995).

[27] A. Schwarz, R. Bhardwaj, Y. Aragane, K. Mahnke, H. Riemann, D. Metze, T. A. Luger, and T. Schwarz, Ultraviolet-B-induced apoptosis of keratinocytes: evidence for partial involvement of tumor necrosis factor-α in the formation of sunburn cells. *Journal of Investigative Dermatology, 104*, 922–927. (1995).

[28] D. Weedon, J. Searle, and J. F. R. Kerr, Apoptosis: its nature and implication for dermatopathology. *American Journal of Dermatopathology, 1*, 133–144. (1979).

[29] A. Ziegler, A. S. Jonason, D. J. Leffell, J. A. Simon, H. W. Sharma, J. Kimmelman, L. Remington, T. Jacks, and D. E. Brash, Sunburn and p53 in the onset of skin cancer. *Nature*, *72*, 773–776. (1994).

[30] R. L. Olson, J. Gaylor, and M. A. Everett, Ultraviolet-induced individual cell keratinization. *Journal of Cutaneous Pathology, 3,* 120–125. (1974).

[31] Y. Gavrieli, Y Sherman, and S. A. Ben-Sasson, Identification of programmed cell death in situ via specific labeling of nuclear DNA fragmentation. *Journal of Cell Biology, 9*, 493–501. (1992).

[32] I. Ito, T. Osaki, S. Ifuku, H. Saimoto, Y. Takamori, S. Kurozumi, T. Imagawa, K. Azuma, T. Tsuka, Y. Okamoto, and S. Minami, Evaluation of the effects of chitin nanofibrils on skin function using skin models. *Carbohydrate Polymers, 101*, 464–470. (2014).

[33] D. N. Ngo and M. M. Kim, Chitin oligosaccharides inhibit oxidative stress in live cells. *Carbohydrate Polymers, 74,* 228–234. (2008).

[34] K. Azuma, T. Osaki, T. Wakuda, S. Ifuku, H. Saimoto, T. Tsuka, T. Imagawa, Y. Okamoto, and S. Minami, Beneficial and preventive effect of chitin nanofibrils in a dextran sulfate sodium-induced acute ulcerative colitis model. *Carbohydrate Polymers, 87*, 1399. (2012).

Figures and tables

Table 1. Composition of test specimens (%)

	1 wt% Ac	HO	35 wt% PG	ANFs	0.2 wt% UCA in 35 wt% PG	0.2 wt% UCA In 30 wt% PG	UNFs	1 wt% SI in 35 wt% PG
Ac cream	50	50						
HO		100						
PG cream		50	50					
ANFs cream	49.59	50		0.41				
UCA cream		50			50			
UNFs cream		50				49.5	0.5	
SI cream		50						50

Ac : Acetic acid, HO : Hydrophilic ointment, PG : Polyethylene glycol, ANFs : Acetic acid chitin nanofibrils, UCA : Urocanic acid, UNFs : Urocanic acid chitin nanofibrils, SI : Squid ink

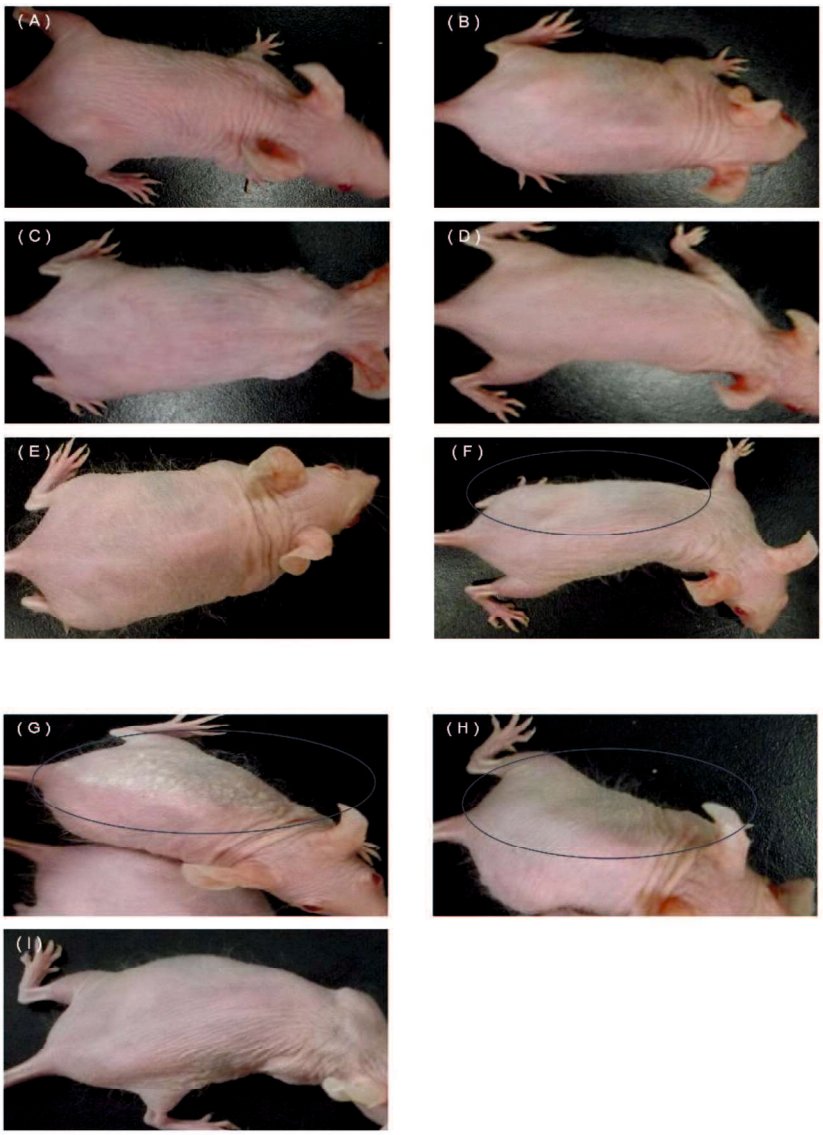

Figure 1. Erythema in hairless mice 12 h after UV irradiation (302 nm, 150 mJ/cm^2)

A: C (+) (non-coated, irradiated) group; B: HO (hydrophilic ointment)-coated group; C: PG (polyethylene glycol) cream-coated group; D: Ac (acetic acid) cream-coated group; E: ANFs (acetic acid chitin nanofibrils) cream-coated group; F: UCA (urocanic acid) cream-coated group; G: UNFs (urocanic acid chitin

nanofibrils) cream-coated group; H: SI (squid ink) cream-coated group; I: C (-) (non-coated and non-irradiated) group. For B–H, each sample was applied to the left side of the mouse's back. The color of the skin on the right and left sides of the mice in the UNA cream group, UCA cream group and Si cream group differed. Contrary to the findings in the C (+) group, UV-irradiation-induced erythema was markedly inhibited in the UNFs cream group as compared to the Si cream group, which was the positive control. The erythema of the UCA cream group was mildly inhibited. The erythema scores for the HO cream, PG cream, Ac cream, and ANFs cream groups were equivalent to the C (+) group. The places surrounded with an oval are the places where erythema is characteristically inhibited.

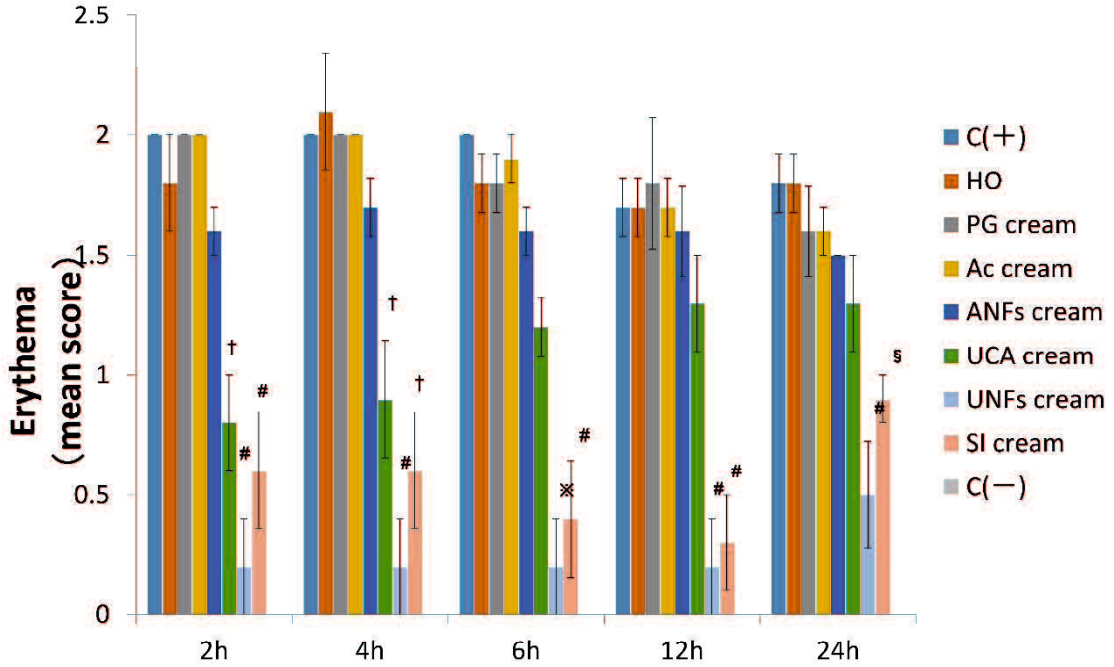

Figure 2. Time-course measurement of cutaneous erythema induced by UV irradiation (302 nm, 150 mJ/cm^2)

C (+) (non-coated, irradiated) group; HO (hydrophilic ointment)-coated group; PG (polyethylene glycol) cream-coated group; Ac (acetic acid) cream-coated group; ANFs (acetic acid chitin nanofibrils) cream-coated group; UCA (urocanic acid) cream-coated group; UNFs (urocanic acid chitin nanofibrils) cream-coated group; SI (squid ink) cream-coated group; and C (-) (non-coated and non-irradiated) group. * $P < 0.01$, significantly different from C (+), HO, PG, Ac, ANFs, and UCA. $^{\#}$ $P < 0.01$, significantly different from C (+), HO, PG, Ac, and ANFs. † $P < 0.01$, significantly different from C (+), HO, PG, and Ac. § $P < 0.01$, significantly different from C (+) and HO. The error bars indicate mean ± SE. (Scheffé's F-test)

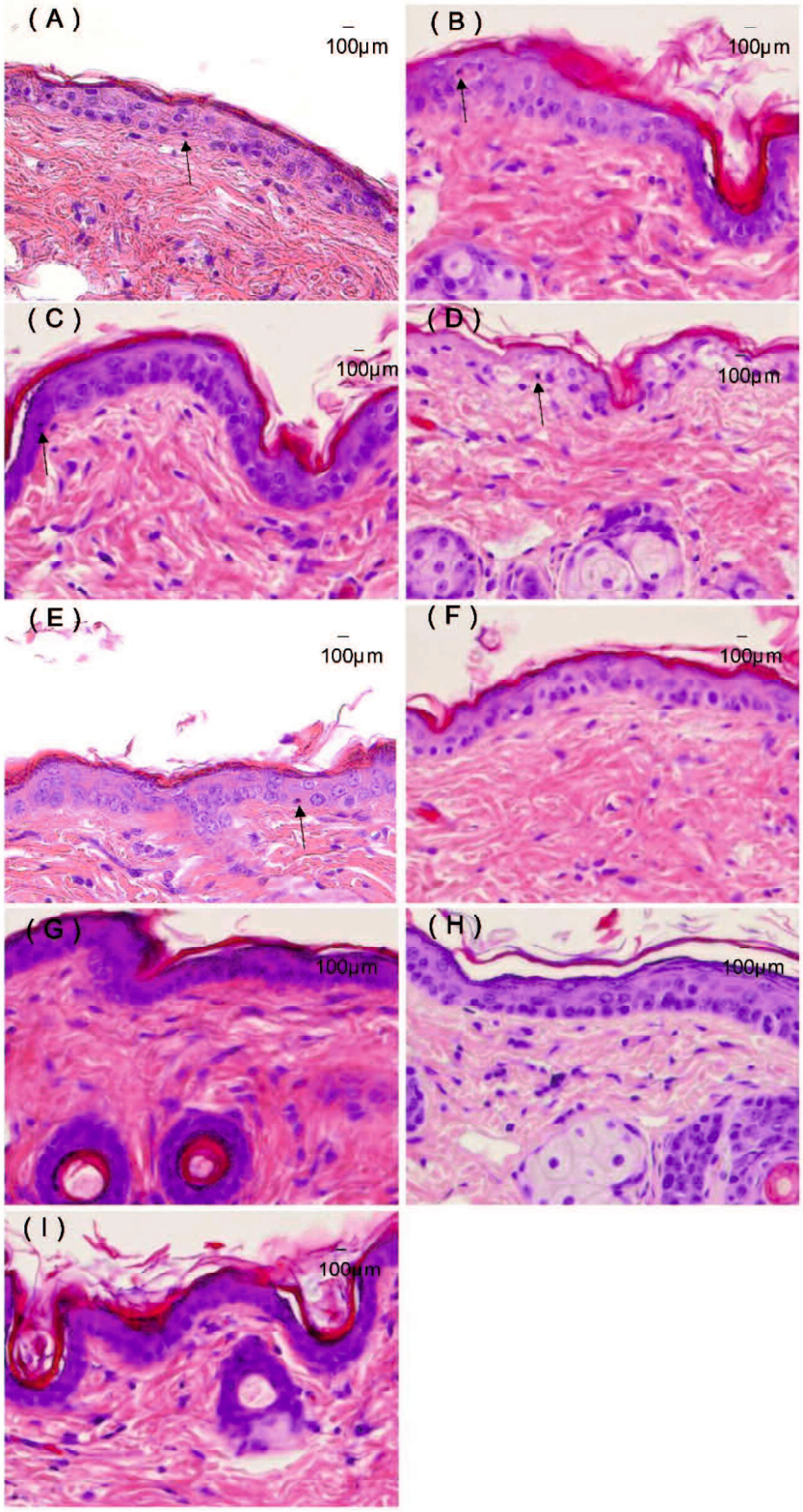

Figure 3. Histology (H&E staining) of the skin of hairless mice 24 h after UV irradiation (302 nm, 150 mJ/cm^2)

A: C (+) (non-coated, irradiated) group; B: HO (hydrophilic ointment)-coated group; C: PG (polyethylene glycol) cream-coated group; D: Ac (acetic acid) cream-coated group; E: ANFs (acetic acid chitin nanofibrils) cream-coated group; F: UCA (urocanic acid) cream-coated group; G: UNFs (urocanic acid chitin nanofibrils) cream-coated group; H: SI (squid ink) cream-coated group; I: C (-) (non-coated and non-irradiated) group. Each specimen was subjected to H&E staining and photographed at a magnification of 400×. Scale bar = 100 μm. The sunburn cell in the epidermis is indicated above the figures with an arrow.

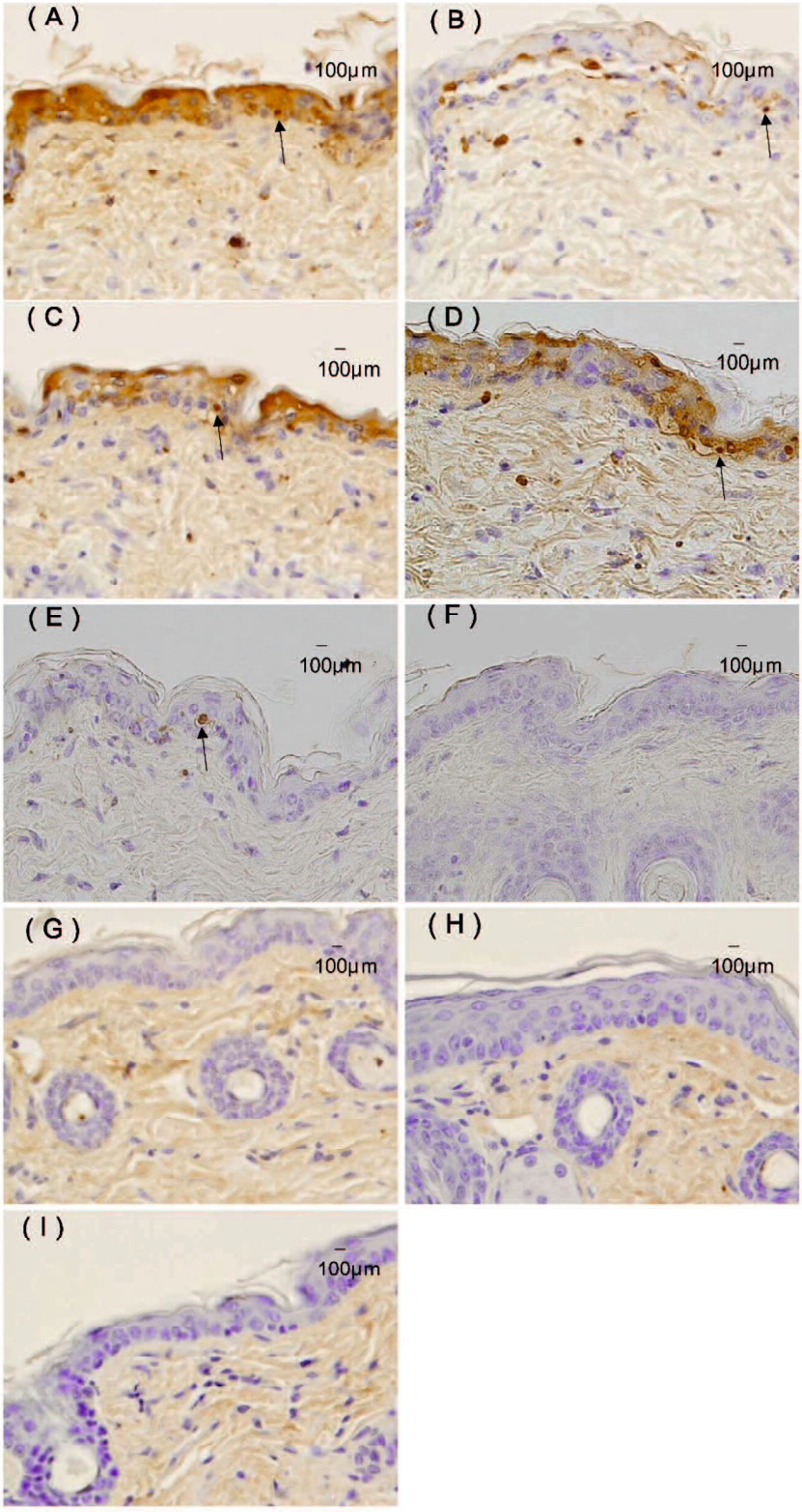

Figure 4. Histology (TUNEL staining) of the skin of hairless mice 24 h after UV irradiation (302 nm, 150 mJ/cm^2)

A: C (+) (non-coated, irradiated) group; B: HO (hydrophilic ointment)-coated group; C: PG (polyethylene glycol) cream-coated group; D: Ac (acetic acid) cream-coated group; E: ANFs (acetic acid chitin nanofibrils) cream-coated group; F: UCA (urocanic acid) cream-coated group; G: UNFs (urocanic acid chitin nanofibrils) cream-coated group; H: SI (squid ink) cream-coated group; and I: C (-) (non-irradiated non-coated) group. Each specimen was subjected to TUNEL staining and was photographed at a magnification of 400×. Scale bar = 100 μm. The sunburn cell in the epidermis is indicated above the figures with an arrow.

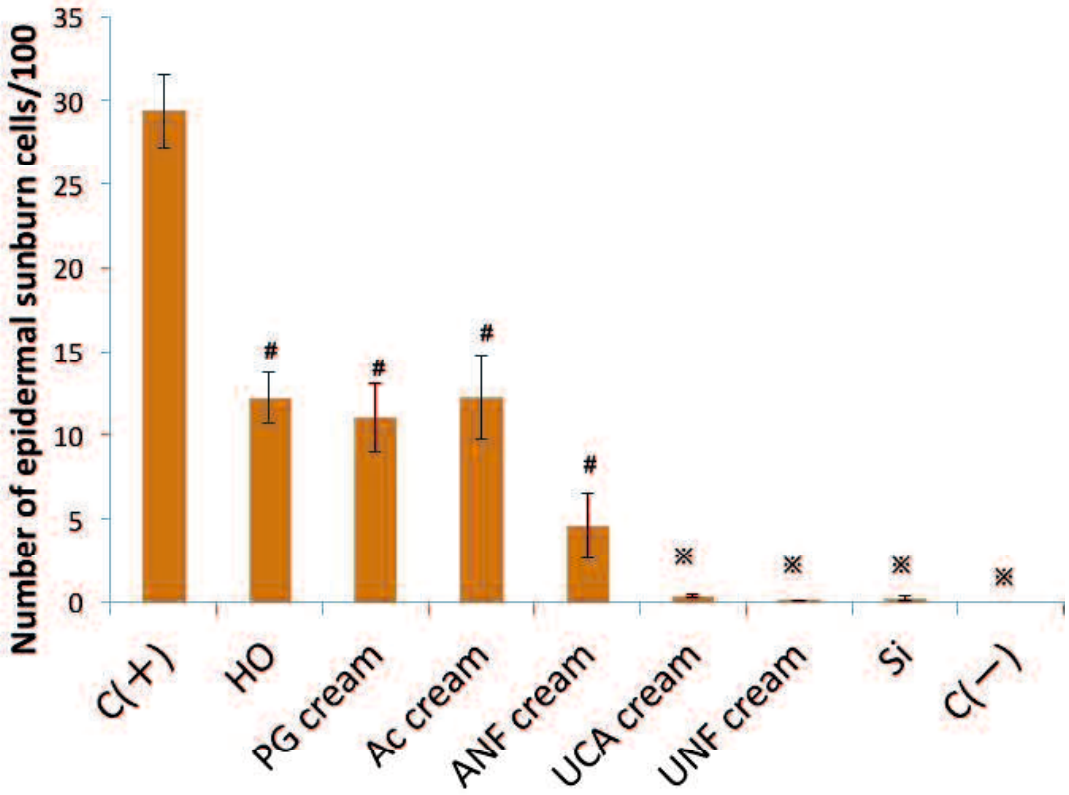

Figure 5. Quantification of sunburn cells in the skin of hairless mice 24 h after UV irradiation (302 nm, 150 mJ/cm^2)

The sunburn cell counts in the UC cream, UNFs cream, SI cream, and C (-) groups were significantly different from those in the C (+), HO, PG cream, and Ac cream groups. The sunburn cell counts in the HO, PG cream, Ac cream, and ANFs cream groups were significantly different from those in the C (+) group. The data shown are the mean ± SE. * $P < 0.01$, significantly different from C (+), HO, PG, and Ac. $^{\#}$ $P < 0.01$, significantly different from C (+), (Scheffé's F-test).

Conclusions

- The results of our study suggested that NFs and NCs protect skin cells while being less inflammatory.

- This study demonstrated that UNFs have a protective effect against UVB irradiation and inhibit UVB irradiation-induced erythema and sunburn cell generation. In addition, the results suggested that NFs itself have a protective effect against UVB.

- A combination of NFs and UCA might show a greater Anti-UV effect than conventional preparations.

Acknowledgments

I would like to express my sincere gratitude to my supervisor, Dr. T Osaki, Associate Professor of Tottori University for providing me this precious study opportunity as a Ph.D student in his laboratory.

I especially would like to express my deepest appreciation to my supervisor, Dr. K Misumi, Professor of Kagoshima University and Dr. Y Okamoto, Professor of Tottori University.

I am very grateful to Dr. H Saimoto, Professor of Tottori University, Dr. S Ifuku, Associate Professor of Tottori University, Dr. S Minami, and Dr. K Azuma, Assistant Professor of Tottori University for their valuable cooperation in my experiments.

This work was supported by a Tottori prefecture-financed aid project for beauty & health products (2011~2012).